



UNIVERSITY OF LEEDS

This is a repository copy of *Combining dispersion modelling with synoptic patterns to understand the wind-borne transport into the UK of the bluetongue disease vector*.

White Rose Research Online URL for this paper:  
<http://eprints.whiterose.ac.uk/112602/>

Version: Accepted Version

---

**Article:**

Burgin, L, Ekström, M and Dessai, S [orcid.org/0000-0002-7879-9364](https://orcid.org/0000-0002-7879-9364) (2017) Combining dispersion modelling with synoptic patterns to understand the wind-borne transport into the UK of the bluetongue disease vector. *International Journal of Biometeorology*, 61 (7). pp. 1233-1245. ISSN 0020-7128

<https://doi.org/10.1007/s00484-016-1301-1>

---

(c) 2017, ISB. This is an author produced version of a paper published in the *International Journal of Biometeorology*. Uploaded in accordance with the publisher's self-archiving policy. The final publication is available at Springer via:  
<https://doi.org/10.1007/s00484-016-1301-1>

**Reuse**

Unless indicated otherwise, fulltext items are protected by copyright with all rights reserved. The copyright exception in section 29 of the Copyright, Designs and Patents Act 1988 allows the making of a single copy solely for the purpose of non-commercial research or private study within the limits of fair dealing. The publisher or other rights-holder may allow further reproduction and re-use of this version - refer to the White Rose Research Online record for this item. Where records identify the publisher as the copyright holder, users can verify any specific terms of use on the publisher's website.

**Takedown**

If you consider content in White Rose Research Online to be in breach of UK law, please notify us by emailing [eprints@whiterose.ac.uk](mailto:eprints@whiterose.ac.uk) including the URL of the record and the reason for the withdrawal request.



[eprints@whiterose.ac.uk](mailto:eprints@whiterose.ac.uk)  
<https://eprints.whiterose.ac.uk/>

1 Combining dispersion modelling with synoptic patterns to  
2 understand the wind-borne transport into the United Kingdom of  
3 the Bluetongue disease vector

4 Laura Burgin<sup>1</sup>, Marie Ekström<sup>2</sup>, Suraje Dessai<sup>3</sup>

5 <sup>1</sup>Met Office, FitzRoy Road, Exeter, EX1 3PB, UK

6 <sup>2</sup>CSIRO Land and Water, Black Mountain, GPO Box 1666, Canberra ACT 2601, Australia 6600

7 <sup>3</sup>School of Earth and Environment, University of Leeds, Leeds, LS2 9JT, UK

8

9 Corresponding author: Marie Ekström, CSIRO Land and Water, Black Mountain, GPO Box 1666,  
10 Canberra ACT 2601, Australia

## 11 Abstract

12 Bluetongue, an economically important animal disease, can be spread over long distances by  
13 carriage of insect vectors (*Culicoides* biting midges) on the wind. The weather conditions which  
14 influence the midge's flight are controlled by synoptic scale atmospheric circulations. A method is  
15 proposed that links wind-borne dispersion of the insects to synoptic circulation through the use of a  
16 dispersion model in combination with principal component analysis (PCA) and cluster analysis. We  
17 illustrate how to identify the main synoptic situations present during times of midge incursions into  
18 the UK from the European continent. A PCA was conducted on high-pass filtered mean sea level  
19 pressure data for a domain centred over north-west Europe from 2005 to 2007. A clustering  
20 algorithm applied to the PCA scores indicated the data should be divided into 5 classes for which  
21 averages were calculated, providing a classification of the main synoptic types present. Midge  
22 incursion events were found to mainly occur in two synoptic categories; 64.8% were associated with  
23 a pattern displaying a pressure gradient over the North Atlantic leading to moderate south-westerly  
24 flow over the UK and 17.9% of the events occurred when high pressure dominated the region  
25 leading to south-easterly or easterly winds. The winds indicated by the pressure maps generally  
26 compared well against observations from a surface station and analysis charts. This technique could  
27 be used to assess frequency and timings of initiations of infection in new areas on seasonal and  
28 decadal timescales, currently not possible with other dispersion or statistical modelling methods.

29

30 **Key words: Bluetongue, *Culicoides*, Wind, Synoptic pattern, Map classification, Dispersion**  
31 **modelling.**

32

## 33 1 Introduction

34 The biting midge *Culicoides* is the principal vector for several viruses causing economically important  
35 animal diseases including Bluetongue (BT), African Horse Sickness and Epizootic Haemorrhagic  
36 Disease. Northern Europe first experienced outbreaks of the disease in 2006 with periodic outbreaks  
37 since. During a peak epidemic in 2007, losses due to death, sickness and reduced productivity of  
38 infected farm animals and movement restrictions applied to infected regions were estimated to be  
39 in the order of many hundreds of millions of pounds (Hoogendam 2007; Wilson and Mellor 2008).

40 The spread of vector-borne diseases is influenced directly and indirectly through a large range of  
41 environmental factors that influence the pathogen, the vector and the host. Development rates,  
42 activity levels, survival, timing of emergence, distributions, abundance levels and migrations of  
43 insect populations are determined to different but significant extents by weather and climate. The  
44 pathogen spread by the vector is itself also regulated by climate, generally replicating at a faster rate  
45 under warmer conditions (Mellor 2000). Other non-climate influences such as farm management  
46 practices and disease-limitation strategies are also relevant if attempting to understand the  
47 mechanisms of disease spread (Tabachnick 2010).

48 Purse *et al.* (2005) suggested that the spread of *Culicoides*-borne diseases into Europe would be  
49 likely to increase under climate change due to several factors; northwards spread of the traditional  
50 Afro-Asiatic vector species as environmental conditions become more habitable, transmission by  
51 indigenous European species becoming viable in warmer temperatures, and overall increased virus  
52 persistence as winters become shorter. If so, it is likely that a modified future climate could lead to  
53 the establishment of new serotypes of BT virus (BTV) and other related viruses in coming decades.  
54 To some extent this prediction has already been confirmed by the rapid spread of BTV type 8 (BTV-8)  
55 through Europe since 2006 and its arrival into the UK in August 2007 (Wilson and Mellor 2008) and  
56 following outbreaks of BTV serotype 1 (BTV-1) and 6 (BTV-6) in the autumn of 2008 in Brittany,  
57 France and the Netherlands respectively.

58 In addition to longer term climatic influences, local, highly variable weather conditions have a  
59 significant impact on midge flight and hence the spread of the viruses (Pedgley, 1982; Purse *et al.*  
60 2005; Carpenter *et al.* 2008). Cold temperatures, high wind speeds and precipitation rates are  
61 known to reduce the number of midges becoming airborne (Blackwell 1997). Midge flight can also  
62 be terminated when they are forced out of the atmosphere by unsuitable weather, such as heavy  
63 rain associated with frontal systems (Sellers and Maafour 1991). Midges are weak fliers due to their  
64 small size of approximately 1-3mm, and will typically undergo short distance flights of less than a

65 kilometre in order to obtain food, shelter or a breeding site (Carpenter *et al.* 2008). But despite  
66 having poor flight abilities, midges can be carried for long distances on the wind (Pedgley 1982).  
67 Therefore, *Culicoides spp.* have been implicated in the spread of the disease into formerly uninfected  
68 areas several hundreds of kilometres away (e.g., Sellers *et al.* 1978; Calistri *et al.* 2004; Alba *et al.*  
69 2004; Gloster *et al.* 2008; Hendrickx *et al.* 2008; Agren *et al.* 2010). Large-scale pressure systems,  
70 controlling wind speed and direction, have previously been linked to patterns of midge-borne  
71 disease spread. For example, outbreaks in Israel have been attributed to carriage of infected midges  
72 from Turkey on winds caused by the Persian trough system (Braverman and Chechik 1996), and the  
73 timing of African Horse Sickness outbreaks in South Africa have been linked to the warm phase of  
74 the El Niño/Southern Oscillation (Baylis *et al.* 1999). In addition to meteorological drivers, Pioz *et al.*  
75 (2012) showed that other important drivers to the velocity of BT spread are elevation (slower in high  
76 elevation) and density of dairy cattle (negatively correlated).

77 In the UK, gradual overland spread of the disease from mainland Europe is prevented by a natural  
78 barrier, the English Channel. Thus incursions of midges only occur at specific times when winds from  
79 mainland Europe are favourable. This study aims to understand how large-scale synoptic conditions  
80 over north-west Europe relate to surface weather conditions during times of midge incursions, giving  
81 insight to the circulation types that are most favourable to midge transport to the UK. Subsequently  
82 this relationship could be used to assess the change in disease risk to the UK, through changes in the  
83 frequency and timing of suitable synoptic conditions, at seasonal and decadal timescales, where  
84 high-resolution wind data necessary to drive a dispersion model may be of limited availability.

85 In this paper, a synoptic map pattern classification and dispersion modelling outputs are combined  
86 in a case study to demonstrate the importance of synoptic circulation conditions for midge transport  
87 across the English Channel. A catalogue of typical mean sea level pressure (MSLP) patterns is created  
88 to characterise daily synoptic circulation patterns for the region then related to midge incursion data  
89 derived from a dispersion model modified to estimate dispersion of 'midge particles' across the  
90 English Channel. Due to the computational expense of the dispersion model, this case study is  
91 limited to a three year period (2005-2007 inclusive). This period covers the first epidemic of the  
92 disease in northern Europe and the first incursion of the disease to the UK. The scope of the paper is  
93 limited to the analysis of wind-borne transport of midges that could potentially act as BT vectors,  
94 across the English Channel into the UK. The dispersion model cannot capture non-meteorological  
95 factors such as the complex short-distance movements of midges across land or human influences  
96 on disease dynamics through animal movements and vaccination programmes. Although some

97 results will be specific for the study site, the overall methodology could be applied to any region  
98 should the appropriate datasets be available.

99

## 100 2 Data

### 101 2.1 Midge days

102 The UK Met Office's numerical atmospheric-dispersion modelling environment (NAME) (Jones *et al.*  
103 2004) has been adapted to simulate the dispersion of wind-borne midges and used to identify days  
104 when midges are likely to be transported from coastal areas of the near-continent to the UK i.e. a  
105 'midge day'. NAME utilises meteorological data from the UK Met Office's operational numerical  
106 weather prediction model, the Unified Model (Davies *et al.* 2005). The midge dispersion model was  
107 developed as part of a web-based early warning system to predict likely incursion events of BTV-  
108 infected midges for the UK government's Department for the Environment, Food and Rural Affairs.  
109 The aim being to identify areas of the UK most at risk of BT outbreaks for use in planning decisions  
110 such as movement restrictions, vaccination schemes and communication programmes to  
111 stakeholders. The service warned of the risk of an incursion into Suffolk overnight of 4/5 August  
112 2007, which is believed to have resulted in the first UK outbreak at Baylham Farm, Ipswich, UK on 22  
113 September 2007 (Gloster *et al.* 2008). This event, along with further testing of the model against  
114 outbreaks in Sweden (Agren *et al.* 2010), validates that the model can accurately simulate midge  
115 incursion events. The mass of 'midge particles' released into the model atmosphere is based on  
116 several meteorological thresholds. These thresholds were derived from the results of experiments  
117 carried out at the Institute for Animal Health, Pirbright, UK (Sanders, C. pers. comm. 2008). No  
118 particles are released when either rainfall exceeds  $1\text{mmhr}^{-1}$ , when wind speed is greater than  $3\text{ms}^{-1}$   
119 or when temperatures are colder than  $3^{\circ}\text{C}$  at the release location, as midges will seek shelter when  
120 the weather is wet, windy or cold. Under suitable conditions particles are released, then advected  
121 following the mean wind with a turbulence component supplied by a random walk scheme. The  
122 'flight' of a midge particle is terminated when rainfall exceeds  $1\text{mmhr}^{-1}$  (washout of the midge), and  
123 also after twelve hours (the estimated maximum flight survival time of a midge (Sanders, C. pers.  
124 comm. 2008).

125 The main midge season is from April to November in northern Europe (Mellor, P. pers. comm. 2008),  
126 thus the model was run on all days during these months for the study period (2005-2007). The  
127 release sites for the midge particles were two locations on the coast of the near-continent,

128 representing possible BT outbreak sites with the potential to cause risk to the UK (Fig. 1). Midge  
129 particles were released during the peak take-off period around sunset (1800-2100Z) and their  
130 positions were tracked for a maximum of 12 hours as they were advected downwind. Days with  
131 midge particles successfully reaching the UK across the English Channel, when the weather was  
132 suitable for midge flight and winds were suitably directed, were classed as a midge day.

133

## 134 2.2 Meteorological data

135 MSLP data from the UK Met Office numerical weather prediction model the Unified Model (Davies *et*  
136 *al.* 2005) at a resolution of 0.11° was used to produce the main patterns of circulation in a domain  
137 from 46°N to 56°N and 13°W to 15°E. This region of Northern Europe was chosen to include the  
138 influence of anticyclonic systems located over Eastern Europe and frontal systems moving in from  
139 the Atlantic on the occurrence of midge days. MSLP grids were extracted for all days in 2005-2007 at  
140 00 UTC to represent the conditions during each overnight midge incursion event.

141 The surface wind climate associated with the main circulation patterns and the midge days was  
142 obtained from weather observations recorded at Langdon Bay, UK (51.13N, 1.35E) (Fig. 1). Hourly  
143 measurements of wind speed and direction at 10m were extracted from the UK Met Office  
144 observation database for the three year period of the study.

145

## 146 3 Methodology

147 To assess if midges require particular synoptic situations to cross the English Channel it was  
148 necessary to elucidate the circulation types that are typical for the region. There are a number of  
149 methods for extracting different modes of variation in the atmosphere in order to relate it to the  
150 surface environment. Manual classifications include the Lamb weather catalogue (Lamb 1972), a  
151 classification of winds over the British Isles into seven basic types and the European  
152 Grosswetterlagen (Hess and Brezovsky 1977), where surface and upper air charts are used to classify  
153 periods of several days into one of three main types of flow; zonal, mixed or meridional. Automated  
154 approaches include correlation based map-pattern classifications, where the similarity between  
155 pressure maps is calculated mathematically to objectively place them in discrete categories (Lund  
156 1963), and eigenvector based classifications.

157 Here an automated methodology outlined by Yarnal (1993) was chosen to ensure a time efficient,  
158 largely objective, and reproducible map pattern classification. This methodology is known as the  
159 circulation-to-environment approach, in which the synoptic classification is produced first and then  
160 related to the environmental variable in question. This approach has been widely used for a variety  
161 of applications; daily precipitation (Serra *et al.* 1998), agricultural wind erosion (Ekström *et al.* 2002),  
162 dust storm frequency (Ekström *et al.* 2004), heavy snowstorms (Esteban *et al.* 2005) and  
163 tropospheric ozone episodes (Hart *et al.* 2006). The map pattern catalogue was then related to  
164 midge days to identify circulation types that are more associated with high risk of trans-channel  
165 transport of midges from the European continent to the UK. The local wind conditions during such  
166 events were then detailed using wind observations from a surface station on the coast of Kent, UK.

167

### 168 3.1 Map pattern classification

169 The automated method used here is an eigenvector-based map pattern classification based on  
170 principal component analysis (PCA) of standardised daily 00UTC MSLP patterns in combination with  
171 a clustering technique, to identify the significant modes of atmospheric circulation across the study  
172 area. The classification procedure involves several steps of analysis, each of which is detailed in the  
173 sections below.

#### 174 3.1.1. High-pass data filtering

175 Prior to the PCA, the MSLP data was subjected to a high pass filter to remove variability on time  
176 scales longer than the typical duration of regional weather systems, as otherwise the PCA would be  
177 dominated by the strong seasonal variability in the pressure data. Unwanted temporal variability in  
178 the data was removed following a method outlined in Hewitson and Crane (1992) whereby  
179 variability on timescale longer than typical weather events are removed through the use of a moving  
180 average filter, preserving variability occurring on timescales less than the first significant harmonic.  
181 Here, to retain the spatial pattern within each daily pressure grid, a time series of average grid  
182 values was created and the moving average filter was applied to these (where the length of the  
183 moving average is the length of the significant harmonic -1 day). The moving average filter was set to  
184 8 day as identified using the tool REDFIT (Schultz and Mudelsee 2002). The difference between the  
185 original grid values and the filtered average time series values was then calculated. These  
186 standardised pressure grids were then used in all the subsequent analyses.



187

188 [3.2.1. Principal component analysis](#)

189 PCA is a technique to reduce the dimensionality of a dataset by retaining those components that  
190 contribute most to its variance, whilst minimising any loss of information (e.g., Jolliffe 2002). PCA is  
191 often used in atmospheric science as a tool to find spatial or temporal variability in physical fields by  
192 condensing a data set into its underlying fundamental modes of variation (e.g., Preisendorfer 1988).

193 The PCA was carried out using the correlation matrix in S-mode decomposition giving spatially  
194 distributed loadings and temporally distributed scores for the selected number of PCs (e.g. Yarnal  
195 1993). The PCA, although strictly a mathematical algorithm, involves elements of subjectivity in the  
196 selection of the number of PCs to retain and whether to rotate the selected PCs or not. The choice of  
197 optimal number of PCs to retain can be aided by a number of different methods. North *et al.* (1982)  
198 provided a rule-of-thumb which proposes that the cut-off should occur where the sampling error of  
199 a particular eigenvalue ( $\lambda$ ) is comparable to or larger than the spacing between  $\lambda$  and a neighbouring  
200 value. The sampling error is given as  $\delta\lambda \sim \lambda(2/N)^{1/2}$ , where N is the number of variables over which  
201 the PCA is carried out on. Two graphical aids, the scree test (Cattell 1966) and the log scree test  
202 (Davis and Kalkstein 1990) have also been used. In the former, the point where the slope of the plot  
203 levels off is assumed to represent the point at which little is added to the explained variance by  
204 adding further PCs, while in the latter a dip in the log-transformed eigenvalue is used as the  
205 indicator.

206 The second element of subjectivity involves whether or not to rotate the retained PCs. Buell (1975)  
207 demonstrated that in S-mode analysis, unrotated PCs give resulting loading maps with regular  
208 characteristic patterns which are statistical artefacts and nearly independent of the spatial variation  
209 in the data. A visual inspection of the unrotated PC loading patterns showed evidence of Buell  
210 patterns, suggesting the need for rotation of the selected PCs. For this application the orthogonal  
211 Varimax rotation (Kaiser 1958) was used. The Varimax transformation changes the relationship  
212 between the components but retains the orthogonality constraint. For a full discussion of the  
213 advantages of rotation see Richmann (1986).

214

### 215 3.1.3. Cluster analysis

216 To group the days with similar characteristics, based on their similarity to the different loading  
217 patterns, the PC scores were submitted to a cluster analysis. Two fundamentally different  
218 approaches can be taken when clustering data depending on the underlying structure of the data;  
219 hierarchical and non-hierarchical cluster analysis (e.g., Wilks 1995). In the former, the analysis  
220 merges subsequent pairs of observations which are most similar in k-dimensional space to build a  
221 hierarchy of sets of groups which tends to work well when there is a natural hierarchical structure to  
222 the data, for example in taxonomy or genetic sequencing. For the map-classification study there was  
223 no reason to assume that the MSLP data had an underlying hierarchical structure hence a non-  
224 hierarchical method was used.

225 Clustering relies on a distance measure to assess the degree of similarity in the PC scores. Here the  
226 method of k-means was used, where  $k$  initial cluster centres are chosen randomly and each  
227 observation is assigned to a cluster based on its Euclidean distance from the cluster centroid. In this  
228 non-hierarchical method the observations are re-assigned to globally optimise the within-cluster  
229 sum of squared distances. To reduce the risk of finding a local minimum the procedure was repeated  
230 100 times with different initial seeds. As the number of clusters is pre-defined the degree of  
231 objectivity in the analysis may be reduced. It was therefore repeated with several different numbers  
232 of clusters ( $k$  was increased from 2 to 20) and the number of clusters chosen was based on two  
233 optimization criteria; the smallest total within-cluster sum-of-squared errors for all clusters and  
234 where the highest number of midge days fitted into one cluster. The spatial characteristics of each  
235 cluster were then represented by a composite of all de-seasonalized grids included in each separate  
236 cluster (e.g. Yarnal 1993).

237 The resulting map-pattern classification was then used to determine if local weather conditions  
238 suitable for midge take-off and subsequent carriage downwind into the UK can be related to larger  
239 scale pressure patterns. This was done by taking the individual pressure pattern for each day that is  
240 classified as a midge-day and determining which cluster it falls within. The summed totals of midge-  
241 day occurrences within each cluster then indicates under which weather regime conditions suitable  
242 for midge take-off and dispersion typically occur.

## 243 4 Results

### 244 4.1 PCA and cluster analysis

245 Guided by the selection procedures outlined in section 3, 5 PCs were retained. The sampling error  
246 and spacing of the eigenvalues are seen to reach the same magnitude at about PC6 (North's rule of  
247 thumb, North *et al.* 1982), (see supplementary material for results from graphical aids). Together,  
248 the 5 retained PCs also explain over 95% of the variance in the dataset (Table 1).

249 The loading patterns of the rotated PCs (RPCs) describe the main modes of variation in the de-  
250 seasonalized pressure grids (Fig. 2). RPC1 displays features of the North Atlantic Oscillation, with  
251 high pressure centred over the Azores and a low pressure system centred over Iceland (Fig. 2a);  
252 RPC2 shows a trough extending from the south-west to the northeast from France through to  
253 Denmark (Fig. 2b); a centre of high pressure situated over the UK dominates the pattern of  
254 variability shown by RPC3 (Fig. 2c); RPC4 (Fig. 2d) shows a distinct high pressure region to the north-  
255 east of the domain, with a low pressure system situated over continental Europe and RPC6 shows  
256 pronounced low pressure in the southeast with a ridge of high pressure extending across the UK (Fig.  
257 2e).

258 The cluster analysis resulted in 5 overall pressure patterns (PPs), subsequently referred to as PP1-  
259 PP5 (Fig. 3). The seasonal and annual relative frequency of each PP, their association with midge  
260 days and persistency are displayed in Table 1.

261 PP1 displays a large area of high pressure over most of the near-continent (Fig. 3a) which would be  
262 expected to generate light south-westerly winds over the English Channel. This PP was found to be  
263 most frequent in winter and to persist for up to six days. The relative frequency of midge days  
264 associated with this PP is very low; annually only 2.2% of midge days are described by this PP.

265 PP2 was the most common pattern annually, with a relative frequency of 34.2%, and shows a  
266 pressure gradient associated with the North Atlantic Oscillation (NAO) over the west of the domain  
267 and high pressure over eastern Europe, leading to south-westerly flow over the UK (Fig 3b). PP2 was  
268 found to occur frequently throughout the year and persist for up to seven days. The largest  
269 proportion of midge days was associated with this PP; 64.8% annually and 62.9%, 65.1% and 65.4%  
270 for spring, summer and autumn respectively.

271 PP3 shows north-westerly flow across the UK, generated by a centre of low pressure system situated  
272 to the north-east of the domain and high pressure in the south-west (Fig 3c). This PP was the second

273 commonest annually during the study period, with an annual relative frequency of 30.1% and it was  
274 found to persist for up to six days. A low number of midge days are associated with this PP, only  
275 7.3% annually.

276 In PP4 a very strong pressure gradient is found across the region, caused by a centre of very low  
277 pressure to the north-west and high pressure in the south-east (Fig 3d). These tight isobars indicate  
278 strong south-westerly winds would be present across the UK. This PP occurred fairly infrequently  
279 throughout the study period, with an annual relative frequency of 9.2%, although it was slightly  
280 more common in winter where it occurred 16.3% of the time. PP4 persisted for up for five days. A  
281 low number of midge days were associated with this PP, only 7.8% annually, although the relative  
282 frequency in autumn was slightly higher at 12.3%.

283 PP5 shows a centre of high pressure situated towards the centre of the region, with a slack gradient  
284 towards lower pressure in the south-east of the domain (Fig 3e). This PP was the third most common  
285 annually, but has the second highest annual relative frequency of midge days at 17.9%. Midge days  
286 were particularly associated with this pattern in spring and summer and are slightly less frequently in  
287 autumn.

288

#### 289 [4.2 Surface climate characteristics of the pressure patterns](#)

290 To verify if the winds indicated by the PPs were representative of the surface conditions,  
291 observations from a station on the south-east coast of England at Langdon Bay have been examined.  
292 These observations also provide some indication of the meteorological characteristics of the airmass  
293 present over the study region. However, differences are expected between the geostrophic winds  
294 and observational data due to the influence of the local environment.

295 Wind roses for each of the PPs are given in Figure 4. In general, there is a good relationship between  
296 the observed wind speeds and directions and the atmospheric circulation expected by examination  
297 of the isobars on the PPs. The wind rose for cluster 1 shows light winds from all directions, as would  
298 be expected in a slack pressure situation described by PP1. The winds for cluster 2 are mainly light to  
299 moderate with southerlies, south-westerlies and westerlies dominating. This corresponds reasonably  
300 well with PP2 which shows south-westerly geostrophic winds over the UK. PP3 indicates north-  
301 westerly winds would be predominant over the UK during dates in this cluster. The wind rose shows  
302 some agreement, with moderate and occasionally strong winds mainly from the west through to the

303 north. The winds on dates in cluster 4 are generally moderate to strong and the wind rose shows a  
304 large dominance in direction from the west, south-west and south. These surface observations  
305 correspond well with the pressure distribution described by PP4, with dense isobars indicating  
306 strong south-westerly winds. Winds at 00UTC during dates in cluster 5 show larger components from  
307 the south, south-east and east and are generally light. There is fairly good correspondence between  
308 these winds and the pressure distribution described by PP5, but a greater north-westerly component  
309 might be expected.

310 The distribution of temperatures at 00UTC for each date in the clusters have also been examined at  
311 Langdon Bay (not shown). Overall, the temperatures typically spanned by each individual cluster  
312 cover a similar range from around -2 to 17°C. Cluster 3 has a slightly larger range from -3 to 19°C, but  
313 the distribution of temperatures within the cluster indicates that it is cooler overall compared to the  
314 other clusters. Clusters 2 and 5 are slightly negatively skewed and show medians that are slightly  
315 warmer than the other clusters at 10 and 11°C indicating slightly warmer temperatures overall on  
316 dates in these clusters. The synoptic conditions represented by clusters 2 and 5 occur more  
317 frequently in spring, summer and autumn, whereas the circulation patterns represented by clusters  
318 1 and 4 occur more often in winter (Table 1). This difference in seasonality combined with  
319 differences in the origin of the airmass may explain why variations are seen in the temperature  
320 statistics for each cluster.

321

#### 322 [4.3 Representation of the synoptic situation on midge days by the map pattern classification](#)

323 Division of the midge days by the cluster analysis resulted in two PPs representing ~83%, of all midge  
324 days. To analyse if these PPs accurately demonstrate the synoptic situation present during midge  
325 incursion events the pressure distribution on midge days in each cluster have been plotted as  
326 composites and analysis synoptic charts on midge days have been examined (Fig 5).

327 The composite maps for midge days in cluster 2 and cluster 5 show similarities to the synoptic  
328 situation described by the map classification for PP2 and PP5. The pressure distribution in PP2 and in  
329 the midge days in cluster 2 are both dominated by a gradient associated with the NAO. However, in  
330 the midge day composite a large area of high pressure is also found in the north east of the domain  
331 over northern Germany. The synoptic situation in both PP5 and in the composite for midge days in  
332 cluster 5 is described by a blocking high. However, the location of the anticyclone differs slightly; it is  
333 located toward Denmark in the midge day composite and is found more centrally in PP5.

334 The representativeness of the composite maps of pressure distribution on midge days in each of the  
335 main clusters have been verified against analysis synoptic charts from the UK Met Office archive. An  
336 example chart for a midge day on 4 Sep 2005 again demonstrates the NAO gradient with high  
337 pressure towards the north east. The chart for a midge day in cluster 5 on 27 Apr 2007 shows that a  
338 large blocking high dominates the weather over the UK in a similar way to the high pressure found in  
339 PP5 and the composite for midge days in cluster 5. Overall some local differences were noted  
340 between the analysis charts and the composites but the general geostrophic flow was found to be  
341 similar in each case.

342

## 343 5 Discussion

344 To enhance understanding of the synoptic conditions conducive to midge incursions across the  
345 English Channel, results from two different analysis techniques are linked, one that categorises the  
346 daily synoptic circulation types and a second that gives the dispersion footprint of midges given a  
347 specific starting point. Because the analysis of MSLP is conducted only on three years of daily data,  
348 the classification is not necessarily robust from a climatology perspective, which would require a  
349 longer time period. Nonetheless, it identified the synoptic types occurring during the three year  
350 period for which this study was conducted. This technique was used to identify the large-scale  
351 atmospheric conditions which are present during times of wind-borne incursions of midges, acting as  
352 vectors for diseases such as BT into the UK from mainland Europe. Two PPs were found to be more  
353 commonly associated with midge days than the others. These showed different attributes in terms  
354 of pressure distribution, airmass characteristics, occurrence in each season and persistency. PP2 is  
355 the most common PP associated with midge days and also the most frequent pattern which occurs  
356 annually over the region. In combination with surface observations of wind speed, wind direction  
357 and temperature it could be deduced that the tropical maritime airmass typically associated with  
358 this pattern would be suitable for the carriage of midges to the UK. Light and moderate south, south-  
359 west and westerly winds were generally present and temperatures were found to be slightly warmer  
360 at these times. Field experiment results show that midges tend to be high in numbers and become  
361 more active during humid, warm weather (Pedgley, 1982; Carpenter *et al.* 2008). They will also not  
362 become airborne during strong winds, but wind of a certain strength is required to carry them across  
363 the English Channel. Therefore, moderate winds create the highest risk situation to coastal areas in  
364 south east England. PP5 also describes synoptic conditions suitable for midge carriage to the UK.  
365 Geostrophic winds determined from the isobars and verified by surface observations show easterly

366 and south easterly winds would be associated with this pressure distribution. Originating from the  
367 continent, this air mass has the potential to create the hottest conditions found in northern Europe.  
368 Temperatures around 25-30°C are ideal for high midge take-off rates. The airborne midges could be  
369 carried to the UK on the gentle and moderate winds associated with the high pressure which  
370 dominates this PP. The other pressure patterns describe situations which are not particularly  
371 suitable for midge take-off and/or transport to the UK. The winds in PP1 were found to be too light  
372 and variable, associated with the slack high pressure over the near continent. In PP3 the northerly  
373 winds are described by the pressure distribution, carrying midges away from the UK. PP4 shows a  
374 strong pressure gradient associated with the NAO. However, this large difference in pressure would  
375 create wind strengths above the threshold for midges to become airborne.

376 The representativeness of the PPs from the map-classification was assessed by comparing these to  
377 composites of the MSLP fields on midge days and analysis charts produced by the UK Met Office. In  
378 general the map-classification was found to be a suitable representation of the synoptic situation  
379 occurring on midge days, but some local differences occurred. These PPs are therefore not suitable  
380 for detailed predictions of locations likely to be at risk in the future, but could be used as a guide to  
381 the frequency and timing of incursion events. Other local effects of, e.g. topography and land/sea  
382 breezes have not been modelled here due to the resolution of the MSLP data. The association  
383 between the PPs and precipitation rates have not been examined here either; moderate to high  
384 rainfall could prevent midges from successfully crossing the English Channel, even if winds are of a  
385 suitable strength and direction. Further, the 3-year period may be too limited to have captured all  
386 the possible synoptic types which occur over the study area and therefore not be a complete  
387 representation of the main pressure distributions in the region.

388 Although this study is limited with regard to general representability of the map pattern  
389 classification, the concept brings insights not demonstrated by existing work on the impact of  
390 weather on the spread of midge-borne diseases. Previous studies to determine the effect of weather  
391 and climate on the spread of insect-borne disease have generally used one of three approaches;  
392 dispersion models, statistical models or process based biological models.

393 Dispersion modelling has typically been carried out on past weather data to determine if wind  
394 carriage of midges from infected areas could be implicated in initiation of new cases of BT (e.g.  
395 Gloster *et al.* 2008; Hendrickx *et al.* 2008; Agren *et al.* 2009; Garcia-Lastra *et al.* 2012 ). Trajectory  
396 models have also been used in a predictive mode to indicate disease spread on short timescales, as  
397 demonstrated by Ducheyne *et al.* (2011) for southern France using a stochastic model drawing on

398 information about weekly wind trajectories, terrain characteristics and epidemiological growth  
399 information. These models have not yet been used to assess the risk of disease spread in a climate  
400 change scenario.

401 Dispersion modelling of insect vectors can also suffer from a lack of suitable methods to directly  
402 verify their results. The NAME model used here has been indirectly validated by showing it can  
403 simulate the pattern and timing of bluetongue outbreaks in previously disease free countries  
404 (Gloster *et al.* 2008; Agren *et al.* 2009). Direct tracking of midge dispersal over tens of metres has  
405 been carried out in a small-scale “mark-recapture” field experiment (Sanders & Carpenter, 2014).  
406 This technique would be near-impossible to carry out on the larger scales involved in midge  
407 incursions into new regions. The quantification of gene flow between insect populations across  
408 regions would inform dispersal routes and therefore virus incursion and spread risks that we have  
409 only been able to describe in a qualitative manner. The imminent publication of the annotated  
410 *Culicoides* genome and second-generation sequencing techniques will allow the calculation of gene  
411 flow between populations across a range of spatial scales and landscapes and determine the  
412 frequency of the wind-borne incursion events described here.

413 A more common approach to study the climate change impacts on species distribution is the use of  
414 ecological niche models, linking species occurrence (through habitat definition) to current patterns in  
415 climate to define the ‘climate envelope’ of the disease (Peters *et al.* 2014). Predictions of where and  
416 when diseases are likely to spread to in the future are then made by determining where the climate  
417 envelope currently exists and/or will be found under future climate change scenarios (Harris *et al.*  
418 2014). Early work using this technique for BT spread used regression models to relate climate  
419 variables to the presence of the vector midge (Baylis *et al.* 2001; Wittmann *et al.* 2001). However,  
420 they assumed only one species of the midge, *Culicoides imicola*, acted as the main vector for the  
421 disease. It has since been shown that more northerly species are capable of transmitting the virus  
422 and each of these species has a different climate envelope (Purse *et al.* 2007). The current northern  
423 European epidemic was initiated in Belgium in 2006, hundreds of kilometres from the nearest  
424 outbreak, from an unknown source. Studies based on the climate envelope of *Culicoides imicola*,  
425 could not have predicted such an event would occur. In a climate change context, Zuliani *et al.*  
426 (2015), ecological niche modelling was used to study the plausible northerly extent of *Culicoides*  
427 *sonorensis* across USA Canada border and Samy and Peterson (2016) used a similar approach, but in  
428 a global context, predicting spatial extension of the disease in central Africa, US and western Russia  
429 under future warmer climates.



430 In biological models the relationships between transmission variables and climate are first  
431 established, and these relationships can then be used to predict rates of spread following an  
432 outbreak (e.g. Gubbins *et al.* 2008). Alternatively, these relationships are used with future climate  
433 scenarios to predict changes in the transmission process. A spatially explicit biological model was  
434 demonstrated by Kelso and Milne (2014) for Australia to study the dispersal of the BT vector  
435 *Culicoides brevitarsis* in Australia. The method also considers wind dispersal of the midge. The  
436 dispersion being informed by relationships derived from 10m wind data with a multiplier  
437 (representing the winds speeds at midge carrying levels), the multiplier being derived from arrival  
438 times at trapping sites for studied events. However, this approach relies on accurate knowledge of  
439 the biology of the disease and its relationship with climate variables, which can vary according to  
440 vector species, host animal and the environment. Also, biological models and ecological niche  
441 models/climate envelope techniques assess the suitability of the climate for vectors and disease  
442 spread once an initial outbreak has occurred. In contrast, the presented technique here can be used  
443 to assess the likely frequency and timing of incursions of disease with explicit representation of  
444 atmospheric dynamics, without which no further spread would occur, no matter how suitable the  
445 climate.

446 Finally, the map-pattern classification developed here is independent of its application. Therefore  
447 the pressure patterns can be related to the occurrence of any other phenomenon thought to be  
448 influenced by large-scale weather systems in the study region. The obvious application would be to  
449 relate the classification to other long-distance midge transport routes across seas in northern Europe  
450 to further aid the assessment of disease spread risk in the region in future seasons and decades.

451

## 452 6 Conclusions

453 This study provides new insight into the relationship between large scale synoptic circulation  
454 patterns and the likelihood for incursions of midges, potentially infected with viruses such as BT, into  
455 the UK from the northern coast of France and Belgium. This relationship assumes the activity levels  
456 and flight paths of the midges are controlled by the characteristics and movements of airmasses,  
457 which are governed by large scale atmospheric flows described by the PPs deduced in this study.

458 Two PPs were found to characterise the synoptic situation present during most midge incursion  
459 events. The main pattern which gives rise to ~65% of all midge days was also the most common  
460 pattern found over northern Europe by the analysis. This PP indicated south-westerly winds over the

461 UK, generally associated with warm, moist tropical maritime air. The other pattern which is  
462 associated with ~18% of midge incursions was found to be fairly infrequent over northern Europe  
463 during the period of the analysis. The winds associated with this pattern were directed from the  
464 continent; airmasses sourced from this region are generally warm and dry. These two patterns  
465 describe synoptic situations suitable for successful midge incursions; warm weather for high take-off  
466 rates and persistent winds towards the UK from the coast of the near-continent.

467 The technique described here could be used to assess changes to the frequency of PPs associated  
468 with midge days on a seasonal or decadal timescale by using simulated MSLP data from climate  
469 models, allowing predictions to be made of the timings and areas at risk in the UK of midge-borne  
470 disease outbreaks. This technique also provides benefits not offered by other modelling techniques,  
471 which do not attempt to assess the transport mechanisms necessary to carry the midge to a new  
472 area and initiate infection.

473

## 474 Acknowledgements

475 The authors gratefully acknowledge comments on the paper from John Gloster, Paul Agnew and  
476 Derrick Ryall at the Met Office, UK, and Anthony Wilson and Christopher Sanders at the Pirbright  
477 Institute, UK. The Atmospheric Dispersion and Air Quality Group at the Met Office, UK is also  
478 thanked for the use of NAME. Laura Burgin was funded by Defra contract SE4204.

479

## 480 References

481 Agren E, Burgin L, Sternberg Lewerin S, Gloster J, Elvander, M. 2010. A likely way of introduction of  
482 BTV8 to Sweden in August 2008 - comparison of results from two models for atmospheric transport  
483 of the biting midge vector. *Veterinary Record* 167: 484-488

484 Alba A, Casal J, Domingo M. 2004. Possible introduction of bluetongue into the Balearic Islands,  
485 Spain, in 2000, via air streams. *Veterinary Record* **155**: 460-461.

486 Baylis M, Mellor PS, Meiswinkel R. 1999. Horse sickness and ENSO in South Africa. *Nature* **397**: 574.  
487 DOI: 10.1038/17512

488 Baylis M, Mellor PS, Wittmann EJ, Rogers DJ. 2001. Prediction of areas around the Mediterranean at  
489 risk of bluetongue by modelling the distribution of its vector using satellite imaging. *Veterinary*  
490 *Record* **149**: 639-643

491 Blackwell, A. 1997. Diel flight periodicity of the biting midge *Culicoides impunctatus* and the effects  
492 of meteorological conditions. *Medical and Veterinary Entomology* **11**: 361-367.

493 Braverman Y, Chechik F. 1996. Air streams and introduction of animal disease borne on *Culicoides*  
494 (Diptera, Ceratopogonidae) into Israel. *Revue Scientifique et Technique de l'Office International des*  
495 *Epizooties* **15**: 1037-1199.

496 Buell CE. 1975. The topography of empirical orthogonal functions. Fourth Conference on Probability  
497 and Statistics in Atmospheric Science, American Meteorological Society: Boston, USA.

498 Calistri P, Giovanni A, Conte A, Nannini D, Santucci U, Patta C, Rolesu S, Caporale V. 2004.  
499 Bluetongue in Italy: part I. *Veterinaria Italiana* **40**: 243-251.

500 Carpenter S, Szymaragd C, Barber J, Labuschagne K, Gubbins S, Mellor PS. 2008. An assessment of  
501 *Culicoides* surveillance techniques in northern Europe: have we underestimated a potential  
502 bluetongue virus vector? *Journal of Applied Ecology* **45**: 1237- 1245. DOI: 10.1111/j.1365-  
503 2664.2008.01511.x

504 Cattell RB. 1966. The scree test for the number of factors. *Multivariate Behavioural Research* **1**: 245-  
505 435.

506 Davies T, Cullen MJP, Malcolm A, Mawson MH, Staniforth A, White AA, Wood N. 2005. A new  
507 dynamical core for the Met Office's global and regional modelling of the atmosphere. *Quarterly*  
508 *Journal of the Royal Meteorological Society* **131**: 1579-1782. DOI: 10.1256/qj.04.101

509 Davis RE, Kalkstein LS. 1990. Development of an automated spatial synoptic climatological  
510 classification. *International Journal of Climatology* **10**: 769-794. DOI: 10.1002/joc.3370100802

511 Ducheyne E, Lange M, Van der Stede Y, Meroc E, Durand B, Hendrickx G. 2011. A stochastic  
512 predictive model for the natural spread of bluetongue. *Preventive Veterinary Medicine* **99**: 48-59

513

514 Garcia-Lastra R, Leginagoikoa I, Plazaola JM, Ocabo B, Aduriz G, Nunes T, Juste RA, 2012. Bluetongue  
515 Virus Serotype 1 outbreak in the Basque country (Northern Spain) 2007-2008. Data support a  
516 primary vector windborne transport. *PLoS ONE* **7**:e34431.doi10.1371/journal.pone.0034421

517 Gloster J, Burgin L, Witham C, Athanassiadou M, Mellor PS. 2008. Bluetongue in the United Kingdom  
518 and northern Europe in 2007 and key issues for 2008. *Veterinary Record* **162**: 298-302.

519 Gubbins S, Carpenter S, Baylis M, Wood JLN, Mellor PS. 2008. Assessing the risk of bluetongue to UK  
520 livestock: uncertainty and sensitivity analyses of a temperature dependent model for the basic  
521 reproduction number. *Journal of the Royal Society Interface* **5**: 363-371. DOI: 10.1098/rsif.2007.1110

522 Ekström M, Jönsson P, Barring L. 2002. Synoptic pressure patterns associated with major wind  
523 erosion events in southern Sweden (1973-1991). *Climate Research* **23**: 51-66.

524 Ekström M, McTainsh GH, Chappell A. 2004. Australian dust storms: temporal trends and  
525 relationships with synoptic pressure distributions (1960-99). *International Journal of Climatology* **24**:  
526 1581-1599. DOI: 10.1002/joc.1072

527 Esteban P, Jones PD, Martín-Vide J, Mases M. 2005. Atmospheric circulation patterns related to  
528 heavy snowfall days in Andorra, Pyrenees. *International Journal of Climatology* **25**: 319-329. DOI:  
529 10.1002/joc.1103

530 Harris RM, Grose MR, Lee G, Bindoff NL, Porfirio LL, Fox-Hughes P. 2014. Climate Projections for  
531 ecologists. *WIREs Clim Change* **5**: 621-637.

532 Hart M, De Dear R, Hyde R. 2006. A synoptic climatology of tropospheric ozone episodes in Sydney,  
533 Australia. *International Journal of Climatology* **26**: 1635-1649. DOI: 10.1002/joc.1332

534 Hendrickx G, Gilbert M, Staubach C, Elbers A, Mintiens K, Gerbier G, Ducheyne E. 2008. A wind  
535 density model to quantify the airborne spread of *Culicoides* species during north-western Europe  
536 bluetongue epidemic, 2006. *Preventive Veterinary Medicine* **87**: 162-181. DOI:  
537 10.1016/j.prevetmed.2008.06.009

538 Hess P, Brezovsky H. 1977. Katalog der Grosswetterlagen Europas (1881-1976). Berichte des  
539 Deutschen Wetterdienstes, Nr. 113 Bd. 15. Selbstverlag des Deutschen Wetterdienstes, Offenbach  
540 am Main.

541 Hewitson BC, Crane RG. 1992. Regional climate in the GISS GCM: Surface air temperature. *Journal of*  
542 *Climate* **5**: 1002–1011.

543 Hoogendam K. 2007. *International study on the economic consequences of outbreaks of bluetongue*  
544 *serotype 8 in north-western Europe*. Van Hall Institute: Leeuwarden, Netherlands

545 Jolliffe IT. 2002. *Principal Component Analysis*. 2nd Edition. Springer-Verlag: New York, USA.

546 Jones A, Thomson D, Hort M, Devenish B. 2007. The U.K. Met Office's next-generation atmospheric  
547 dispersion model, NAME III. In: Borrego C, Norman AL. (Eds) *Air Pollution Modeling and its*  
548 *Application XVII*, Springer, New York, USA

549 Kaiser HF. 1958. The varimax criterion for analytic rotation in factor analysis. *Psychometrika* **32**: 443-  
550 482.

551 Kelso JK, Milne GJ. 2014. A spatial simulation model for the dispersal of the Bluetongue vector  
552 *Culicoides brevitarsis* in Australia. *PLOS ONE* **9**(8): e104646. DOI:10.1371/journal.pone.0104646.

553 Lamb HH. 1972. British Isles weather types and a register of the daily sequence of circulation types.  
554 *Geophysical Memoirs 16*, HMSO: London, UK

555 Lund IA. 1963. Map-pattern classification by statistical methods. *Journal of Applied Meteorology* **2**:  
556 56-65.

557 Mellor, P.S. 2000. Replication of arboviruses in insect vectors. *Journal of Comparative*  
558 *Pathology* **123**: 231-247.

559 North GR, Bell TL, Cahalan RF, Moeng FJ. 1982. Sampling errors in the estimation of empirical  
560 orthogonal functions. *Monthly Weather Review* **110**: 699-706.

561 Pedgley D. 1982. *Windborne pests and diseases*. Ellis Horwood Limited: Chichester, UK.

562 Preisendorfer RW. 1988. *Principal component analysis in meteorology and oceanography*. Elsevier:  
563 Amsterdam, The Netherlands

564 Peters J, Waegeman W, Van doninck J, Ducheyne E, Calvete C, Lucientes J, Verhoest NEC, De Baets B.  
565 2014. Predicting spatio-temporal distributions in Spain based on environmental habitat  
566 characteristics and species dispersal. *Ecological Informatics* **22**: 69-80.

- 568 Pioz M, Guis H, Crespin L, Gay E, Calavas D, Durand B, Abrial D, Ducrot C, 2012. Why did Bluetongue  
569 spread the way it did? Factors influencing the velocity of Bluetongue Virus Serotype 8 Epizootic  
570 Wave in France? *PLoS ONE* **7**: e43360. Doi:10.1371/journal.pone.0043360Purse BV, Mellor PS,  
571 Rogers DJ, Samuel AR, Mertens PC, Baylis M. 2005. Climate change and the recent emergence of  
572 bluetongue in Europe. *Nature Reviews Microbiology* **3**: 171-181. DOI: 10.1038/nrmicro1090
- 573 Purse BV, McCormick BJJ, Mellor PS, Baylis M, Boorman JPT, Borrás D, Burgu I, Capela R, Caracappa  
574 S, Collantes F, De Liberato C, Delgado JA, Denison E, Georgiev G, El Harak M, De La Rocque S, Lhor Y,  
575 Lucientes J, Mangana O, Miranda MA, Nedelchev N, Nomikou K, Ozkul A, Patakakis M, Pena I,  
576 Scaramozzino P, Torina A, Rogers DJ. 2007. Incriminating bluetongue virus vectors with climate  
577 envelope models. *Journal of Applied Ecology* **44**: 1231-1242. DOI: 10.1111/j.1365-2664.2007.01342.x
- 578 Richman MB. 1986. Rotation of principal components. *Journal of Climatology* **6**: 293-335
- 579 Sanders CJ, Carpenter S. 2014. Assessment of an immunomarking technique for the study of  
580 dispersal of *Culicoides* biting midges. *Infection, Genetics and Evolution* **28**: 583-587
- 581 Samy AM, Peterson AT. 2016. Climate change influences on the global potential distribution of  
582 Bluetongue Virus. *PLOS ONE* **11**(3):e0150489. DOI:10.1371/journal.pone.0150489.
- 583 Schultz M, Mudelsee M. 2002. REDFIT: estimating red-noise spectra directly from unevenly spaced  
584 paleoclimatic time series. *Computers and Geosciences* **28**: 421-426
- 585 Sellers RF, Pedgley DE, Tucker MR. 1978. Possible windborne spread of bluetongue to Portugal, June-  
586 July 1956. *Journal of Hygiene* **81**: 189-196.
- 587 Sellers RF, Maarouf, AR. 1991. Possible introduction of Epizootic Hemorrhagic-Disease of Deer Virus  
588 (serotype-1) and Bluetongue Virus (serotype-11) into British-Columbia in 1987 and 1988 by infected  
589 *Culicoides* carried on the wind. *Canadian Journal of Veterinary Research*. **55**: 367-370
- 590 Serra C, Fernandez Mills G, Periago MC, Lana X. 1998. Surface synoptic circulation and daily  
591 precipitation in Catalonia. *Theoretical and Applied Climatology* **59**: 29-49. DOI:  
592 10.1007/s007040050011
- 593 Tabachnick WJ. 2010. Challenges in predicting climate and environmental effects on vector-borne  
594 disease epistystems in a changing world. *The Journal of Experimental Biology* **213**: 946-954.

595 Wilks DS. 1995. *Statistical methods in the atmospheric sciences*. Academic Press: London, UK.

596 Wilson A, Mellor P. 2008. Bluetongue in Europe: Vectors, epidemiology and climate change.  
597 *Parasitology Research* **103**: S69-S77. DOI: 10.1007/s00436-00008-01053-x.

598 Wittmann EJ, Mellor PS, Baylis M. 2001. Using climate data to map the potential distribution of  
599 *Culicoides imicola* (Diptera: Ceratopogonidae) in Europe. *Revue Scientifique et Technique de l'Office*  
600 *International des Epizooties* **20**: 731-740

601 Yarnal B. 1993. *Synoptic climatology in environmental analysis*. Belhaven Press: London, UK

602 Zuliani A, Massolo A, Lysyk T, Johnson G, Marshall S, Berger K, Cork SC. 2015. Modelling the  
603 northward expansion of *Culicoides sonorensis* (Diptera: Ceratopogonidae) under future climate  
604 scenarios. *PLOS ONE* **10**(8): e0130294. DOI:10.1371/journal.pone.0130294

605

606

607

608

609

610

611

612 Table 1. Results of PCA and PP analysis. First section shows results of the PCA followed by the  
613 seasonal and annual relative frequency distribution of each PP and seasonal and annual relative  
614 frequency distribution of midge days associated with each PP ( here  $N$  is the number of observations  
615 in each season and for the whole year). Last five rows gives relative frequency of PP persistency  
616 (here  $N$  is the total number of days in each cluster).

| PCA results                                 |            |      |                    |      |      |                                   |     |     |
|---|------------|------|--------------------|------|------|-----------------------------------|-----|-----|
| PC  | Eigenvalue |      | Explained variance |      |      | Cumulative explained variance (%) |     |     |
| 1   | <b>1</b>   |      | <b>1314.6</b>      |      |      | <b>48.6</b>                       |     |     |
| 2   | <b>2</b>   |      | <b>848.4</b>       |      |      | <b>29.6</b>                       |     |     |
| 3   | <b>3</b>   |      | <b>648.5</b>       |      |      | <b>10.2</b>                       |     |     |
| 4   | <b>4</b>   |      | <b>478.7</b>       |      |      | <b>4.6</b>                        |     |     |
| 5   | <b>5</b>   |      | <b>273.2</b>       |      |      | <b>2.4</b>                        |     |     |
| 6   | 6          |      | 117.0              |      |      | 1.2                               |     |     |
| 7   | 7          |      | 102.9              |      |      | 0.7                               |     |     |
| 8   | 8          |      | 73.4               |      |      | 0.5                               |     |     |
| 9   | 9          |      | 51.6               |      |      | 0.4                               |     |     |
| 10  | 10         |      | 17.0               |      |      | 0.3                               |     |     |
| Relative frequency of PPs (%)               |            |      |                    |      |      |                                   |     |     |
| PP  | DJF        | MAM  | JJA                | SON  | YEAR |                                   |     |     |
| 1   | 14.8       | 6.5  | 2.2                | 5.9  | 7.3  |                                   |     |     |
| 2   | 28.5       | 33.3 | 32.6               | 42.5 | 34.2 |                                   |     |     |
| 3   | 25.6       | 33.3 | 39.9               | 21.6 | 30.1 |                                   |     |     |
| 4   | 16.3       | 7.2  | 4.3                | 9.2  | 9.2  |                                   |     |     |
| 5   | 14.8       | 19.6 | 21.0               | 20.9 | 19.1 |                                   |     |     |
| N   | 270        | 276  | 276                | 273  | 1095 |                                   |     |     |
| Relative frequency of midge days per PP (%) |            |      |                    |      |      |                                   |     |     |
| PP  | DJF        | MAM  | JJA                | SON  | YEAR |                                   |     |     |
| 1   | 0          | 2.9  | 0                  | 3.7  | 2.2  |                                   |     |     |
| 2   | 0          | 62.9 | 65.1               | 65.4 | 64.8 |                                   |     |     |
| 3   | 0          | 8.6  | 11.1               | 3.7  | 7.3  |                                   |     |     |
| 4   | 0          | 5.7  | 3.2                | 12.3 | 7.8  |                                   |     |     |
| 5   | 0          | 20.0 | 20.6               | 14.8 | 17.9 |                                   |     |     |
| N   | 0          | 35   | 63                 | 81   | 179  |                                   |     |     |
| Relative frequency of PP persistency (%)    |            |      |                    |      |      |                                   |     |     |
| Increasing nb of days →                     | 1          | 2    | 3                  | 4    | 5    | 6                                 | 7   | N   |
| PP1   | 12.5       | 6.3  | 5.0                | 3.8  | 1.3  | 1.3                               |     | 80  |
| PP2   | 16.3       | 8.3  | 4.8                | 2.1  | 1.3  | 0.5                               | 0.2 | 375 |
| PP3   | 18.2       | 11.2 | 4.2                | 2.4  | 0.0  | 1.2                               |     | 330 |
| PP4   | 14.9       | 4.0  | 6.9                | 4.0  | 2.0  |                                   |     | 101 |
| PP5   | 19.1       | 11.5 | 9.6                | 3.3  | 1.4  |                                   |     | 209 |

617

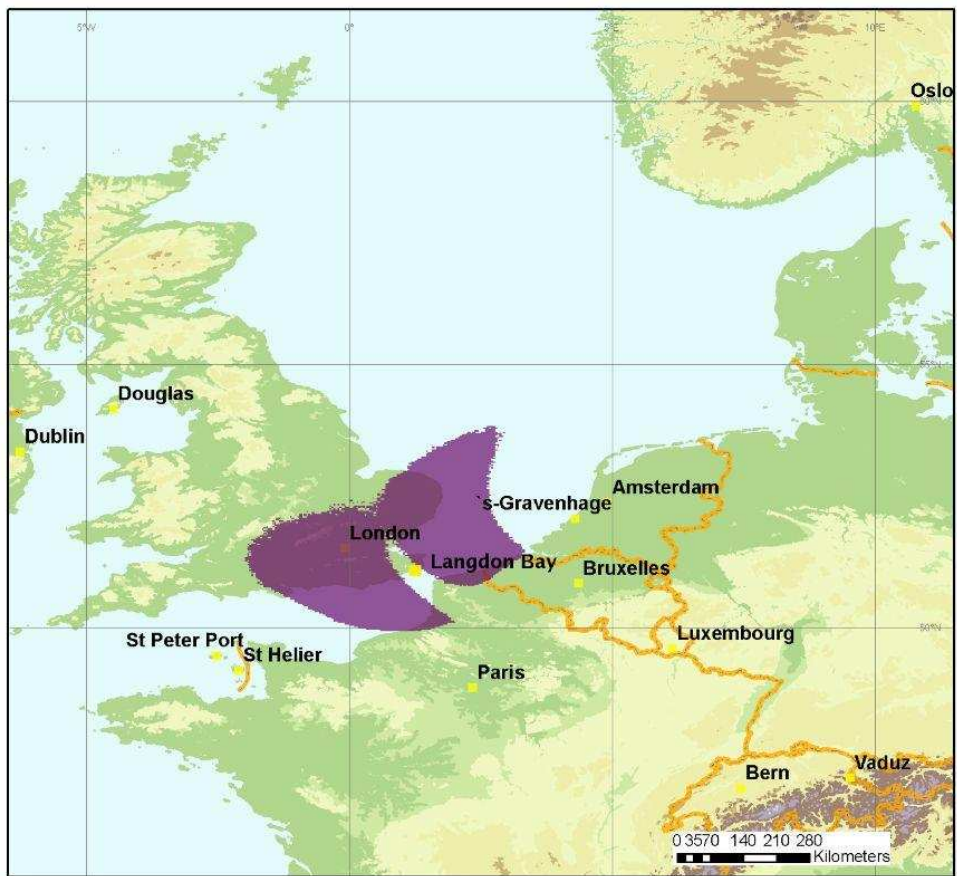
618

619

620

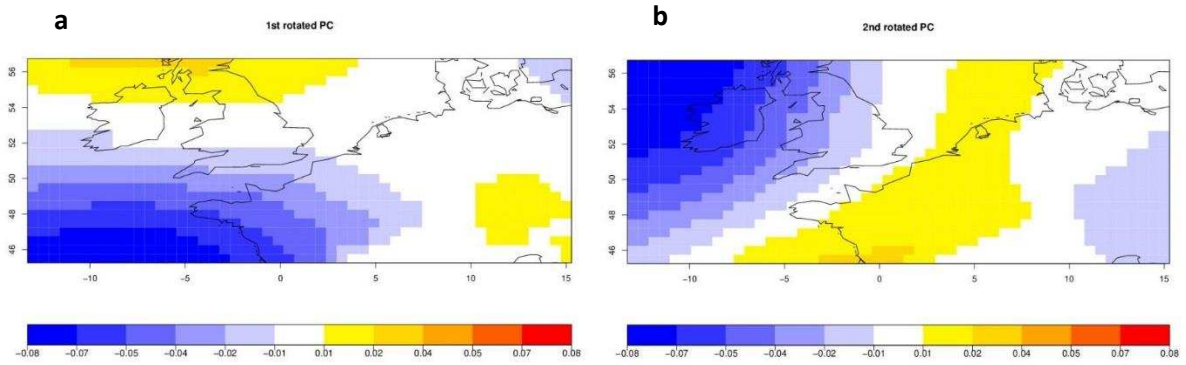


621 Figure 1. Example of output from the NAME model used to determine 'midge days'.

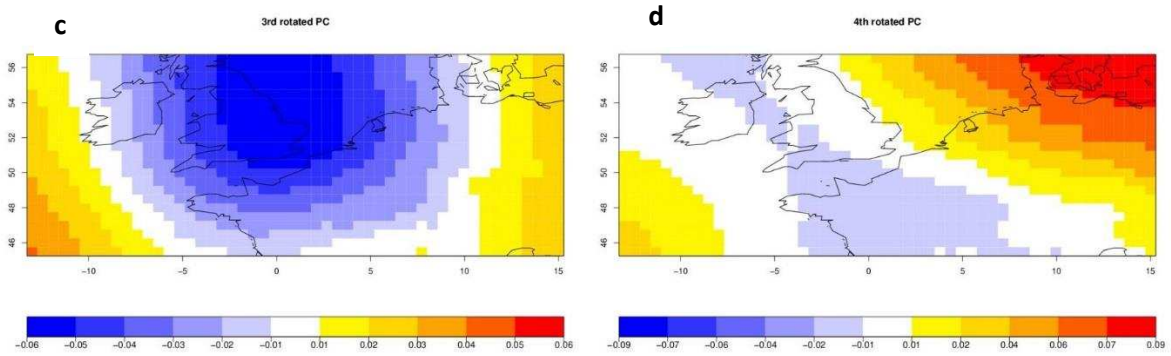


622

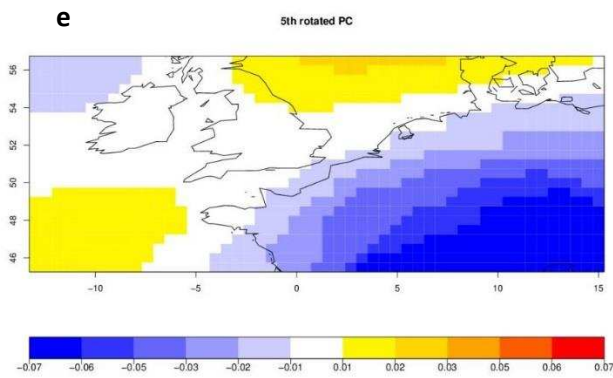
623 Figure 2. Loading patterns of the first five RPCs (a-e).



624



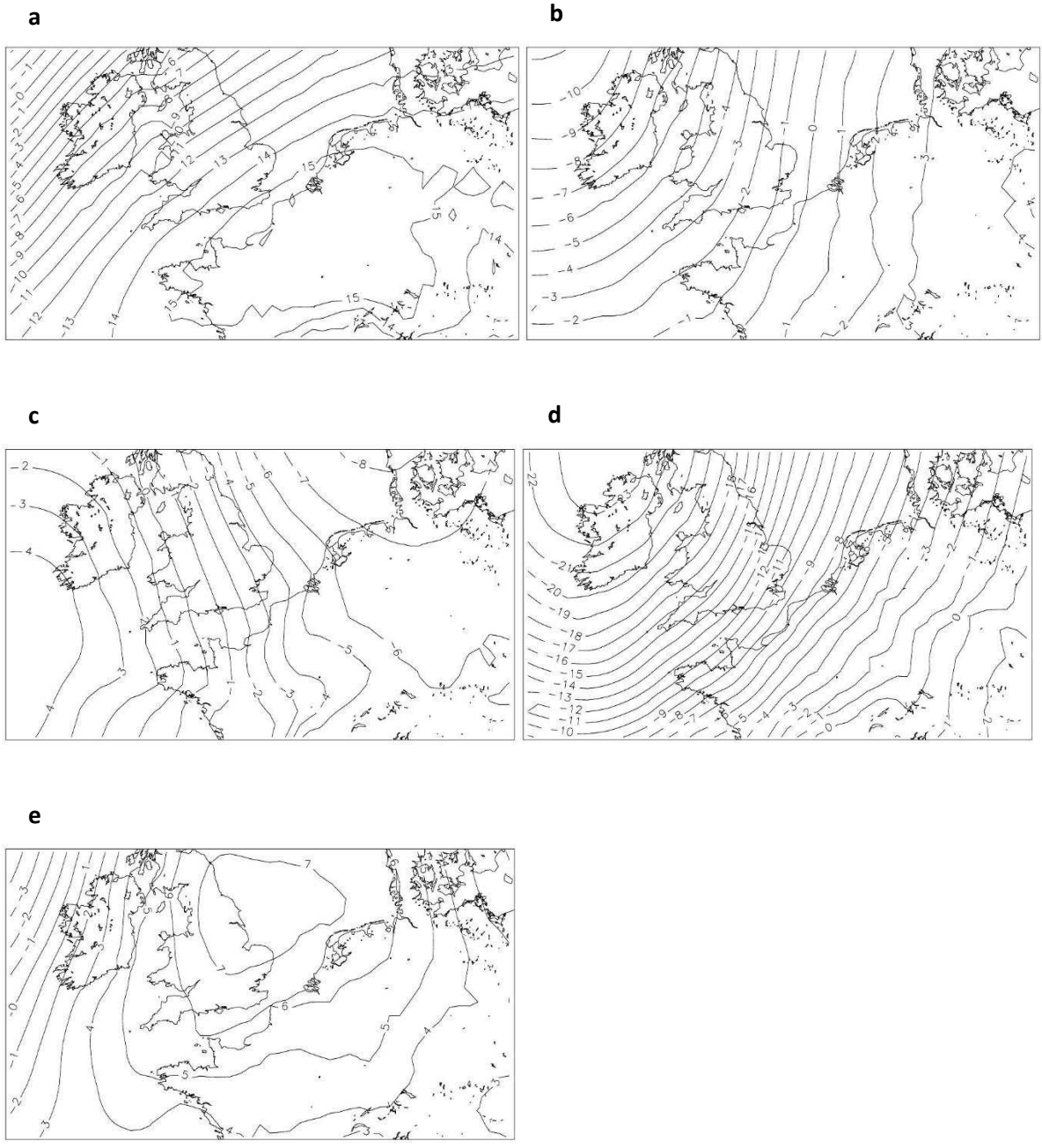
625



626

627

628 Figure 3: Average de-seasonalized pressure patterns (hPa) for each cluster (a-e).



629

630

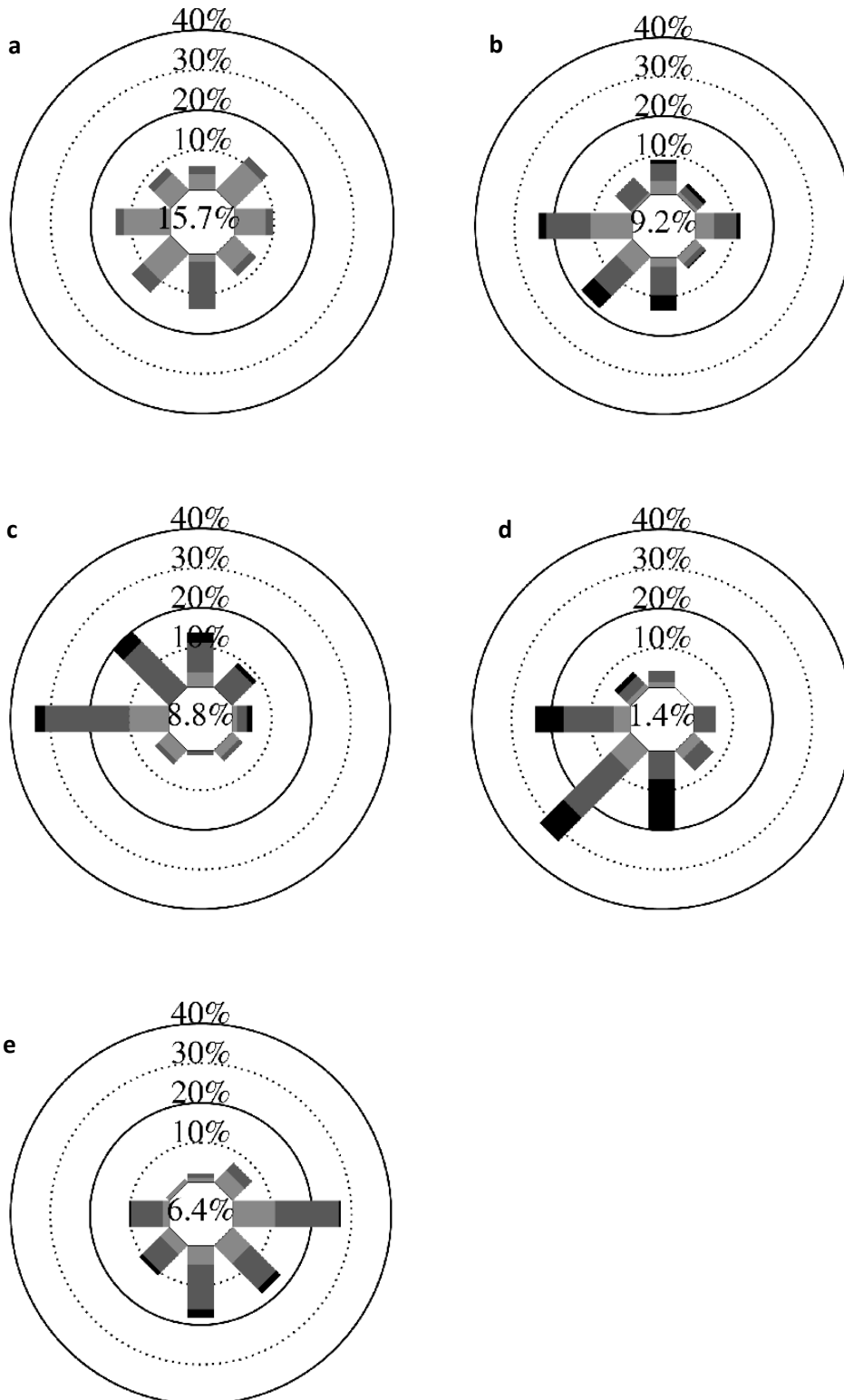
631

632

633 Figure 4: Windroses showing wind speed and direction at 00UTC for clusters 1-5 (a-e) at Langdon Bay.

634 Light-grey=1-5ms<sup>-1</sup>, mid-grey=5-10ms<sup>-1</sup>, black=greater than 10ms<sup>-1</sup>, number of calms (less than 1ms<sup>-1</sup>)

635 shown as a percentage in the centre.



636

637

638

639 Figure 5: Composite MSLP patterns for all midge days in cluster 2 (a) and cluster 5 (c) and example  
640 synoptic charts for a midge day in cluster 2 (04/09/05) (b) and cluster 5 (27/04/07) (d).

